



Climate of Syria Based on Cordex Simulations: Present and Future

Nour Naaouf¹ · Csaba Zsolt Torma²

Received: 5 November 2022 / Revised: 7 August 2023 / Accepted: 13 August 2023 / Published online: 11 September 2023
© The Author(s) 2023

Abstract

Regional climate models are widely used to assess current and future impacts of climate change. In this study, we evaluate the performance of regional climate models from the Coordinated Regional Climate Downscaling Experiment programme integrated over the following three CORDEX domains: AFR, MNA and WAS. Four meteorological variables (temperature, precipitation, solar radiation and cloud cover) were evaluated over Syria at a grid spacing of 0.44°. The performance of five models in simulating the present climate characteristics (1989–2008) is evaluated with respect to the observations: CRU, ERA5 reanalysis and SARA and CLARA satellite data. We find that the mini-ensemble captures well the general spatial patterns and annual cycles of the selected variables. Another aim of this study was to assess the expected change of the mentioned four climate variables over Syria under the moderate emission scenario (RCP4.5) and the high emission scenario (RCP8.5) in the near future (2031–2050) and in the far future (2080–2099) with respect to the present climate (1989–2008). The simulations show a decreasing trend in cloud cover (between 6% and 10%) and precipitation (up to 9%) by mid and late century, regardless of the forcing scenarios. The simulations show a pronounced warming over Syria, which is expected to reach 6 °C by the end of the twenty-first century following the high greenhouse gas concentration scenario (RCP8.5). Furthermore, such an increase, combined with a decrease in precipitation, will shift Syria's climate towards a more arid one.

Keywords Future projections · CORDEX–CORE · MNA · AFR · WAS · TAS · RDS · CLT · PR · Syria

1 Introduction

On one hand, climate models can be useful tools for providing information on human-induced climate change (IPCC 2013), but on the other hand, the climate parameters derived from climate model simulations are subject to high uncertainties. Indeed, climate models are characterised by biases compared to observations (Torma et al. 2011; Kotlarski et al. 2014). Consequently, both types of climate models, global and regional (GCM and RCM, respectively), can only provide information on climatic conditions with uncertainties. Climate models can be seen as imperfect tools that cannot

predict the future with certainty, but they can provide useful information that serves as a fundamental pillar for making decisions about mitigating or adapting to climate change (King et al. 2015; Sutton 2019).

Global warming is real, and the predictions about the climate have to be taken seriously (Saravanan 2002). In December 2015, almost all of the world's nations agreed in Paris, France, on how to tackle the climate crisis. The aim of this agreement, known as the Paris Agreement, is to keep the global average temperature rise well below 2 °C, and ideally below 1.5 °C to reduce the risks and the impacts of climate change (IPCC 2015; Betts et al. 2018; Dudley and Suding 2020).

The observed temperature changes are not uniform: the increase is more pronounced over land (1.59 °C) than over the ocean (0.88 °C). Based on observations and proxy data, global surface temperature has risen faster since 1970 than in any other 50-year period in at least the last 2000 years (IPCC 2023). Anthropogenic climate change has also been implicated in ecosystem impacts from slow-onset processes, such as ocean acidification, sea-level rise or regional decreases in precipitation, which have contributed to desertification

✉ Nour Naaouf
naaouf@student.elte.hu

Csaba Zsolt Torma
csaba.zsolt.torma@ttk.elte.hu

¹ Institute of Cartography and Geoinformatics, ELTE Eötvös Loránd University, Budapest, Hungary

² Department of Meteorology, ELTE Eötvös Loránd University, Institute of Geography and Earth Sciences, Budapest, Hungary

and exacerbated land degradation, particularly in low-lying coastal areas, river deltas, drylands and permafrost areas. Nearly, 50% of coastal wetlands have been lost in the last 100 years as a result of the combined effects of local human pressures, sea-level rise, warming and extreme climate events (IPCC 2023). The frequency and intensity of climate extremes are considered more sensitive indicators of climate warming than mean climate values, and these extremes are often associated with significant impacts on natural and human systems (Zheng et al. 2019). An increase in climate extremes could lead to direct or indirect health impacts through food insecurity (Betts et al. 2018), natural disasters (Sun et al. 2019), challenges to the global energy system (Meng et al. 2020; Yang et al. 2020), and increased global conflict (Harari and Ferrara 2018).

Assessing current and future climate characteristics is important for developing long-term adaptation and mitigation strategies around the world as a response to climate change (Forster et al. 2020; Abbass et al. 2022).

Considering that Syria is already exposed to natural hazards (ACSAD 2011; Massoud 2010) and suffers from an ongoing armed conflict, adaptation and mitigation strategies must be prepared to address the impacts of climate change in a country that is heavily dependent on the agriculture (45% of the population depends on agriculture for their livelihoods (FAO 2021)).

RCMs are widely used in the regional assessment of the impacts of climate change (Giorgi 2019; Tapiador et al. 2020). It is important to assess the performance of individual models in describing climatic conditions before using their output for impact assessment (Giorgi and Bi 2000; Hassan et al. 2015; Diro and Sushama 2017; Ozturk et al. 2018).

Addressing the vulnerability of the Middle Eastern countries including Syria related to drought and climate change has been one of the research priorities in recent years (Faour et al. 2010; Massoud et al. 2010; Karnieli et al. 2019; Kelley et al. 2015).

In the last decade, several studies (Almazroui et al. 2012, 2017, 2020) have used different climate models to assess the future climate change and associated uncertainties over the Arabian Peninsula, which includes the Syrian territory, where future changes are assessed based on GCM simulations (Coupled Model Intercomparison Project Phase 5 and 6: CMIP5 (Taylor et al. 2012) and CMIP6 (Eyring et al. 2016)).

A great contribution to the climate studies over Syria was made by Prof. Dr. Ali Hassan Mousa (in Arabic, e.g., climate changes, contemporary issues in climate, applied climatology and bioclimatology; Mousa 2011). His work has mainly focused on the erratic atmospheric conditions that have prevailed in Syria over the past few years, leading to unusual rainfall that has occurred mainly in the interior of Syria. In addition, the papers discussed the atmospheric factors and

local causes that led to major flooding and inundation, causing loss of property and lives, and soil erosion.

The Arab Center for the Studies of Arid zones and Dry lands ((ACSAD), <https://acsad.org/en/>), established in Damascus in 1968, conducts research and studies related to agricultural development, drought mitigation and resilience, and is considered as one of the leading innovators in this field. Other climate change-related studies have also been conducted by FAO (Food and Agriculture Organization of the United Nations, FAO 2021) and also by RICCAR (Regional Initiative for the assessment of Climate Change impacts on water resources and socio-economic vulnerability in the Arab Region, ESCWA 2017).

This study is one of the first to focus on the climate and projected climate change over the region of Syria and its surroundings. A central objective of this research is to contribute to the development of climate change adaptation and mitigation strategies in Syria. The next section provides background information on the study area, followed by sections detailing the data and methods, and presenting the performance of the models in simulating the mean climate over Syria. The paper concludes with a discussion of projected changes in the selected variables (temperature, precipitation, solar radiation and cloud cover).

2 Description of the Study Area

In this research, we provide the assessment of the aforementioned outputs of models at medium resolution (50 km grid spacing) using a set of climate simulations accomplished by five RCMs integrated over three CORDEX domains: MENA, WAS and the AFR CORDEX regions (MENA: the Middle East and North Africa, WAS: Western Asia and AFR: Africa). Figure 1 depicts the CORDEX regions covering the region of interest (Syria).

Syria is a country which has an area of 185,180 km² and is located on the eastern side of the Mediterranean (Fig. 2). The interior part of the country is occupied mainly by a plateau, at an altitude of between 400 and 1200 m, with a combination of arid and semi-arid environments. Most of the Syria's territory is covered by the Syrian desert (located in the central and south-eastern parts of the country).

Natural forests cover about 2% of the country and water bodies cover less than 1% of the country (FAO 2014). Most of the country receives very little rainfall; over about 60% of the country the average annual precipitation is less than 250 mm. Syria has four geographical zones: the Mediterranean coast to the west, mountains to the east of the coast, steppe to the east of the mountains and along the northern border, and desert along the south-eastern borders with Jordan and Iraq (United States Agency for International Development (USAID) 2017).

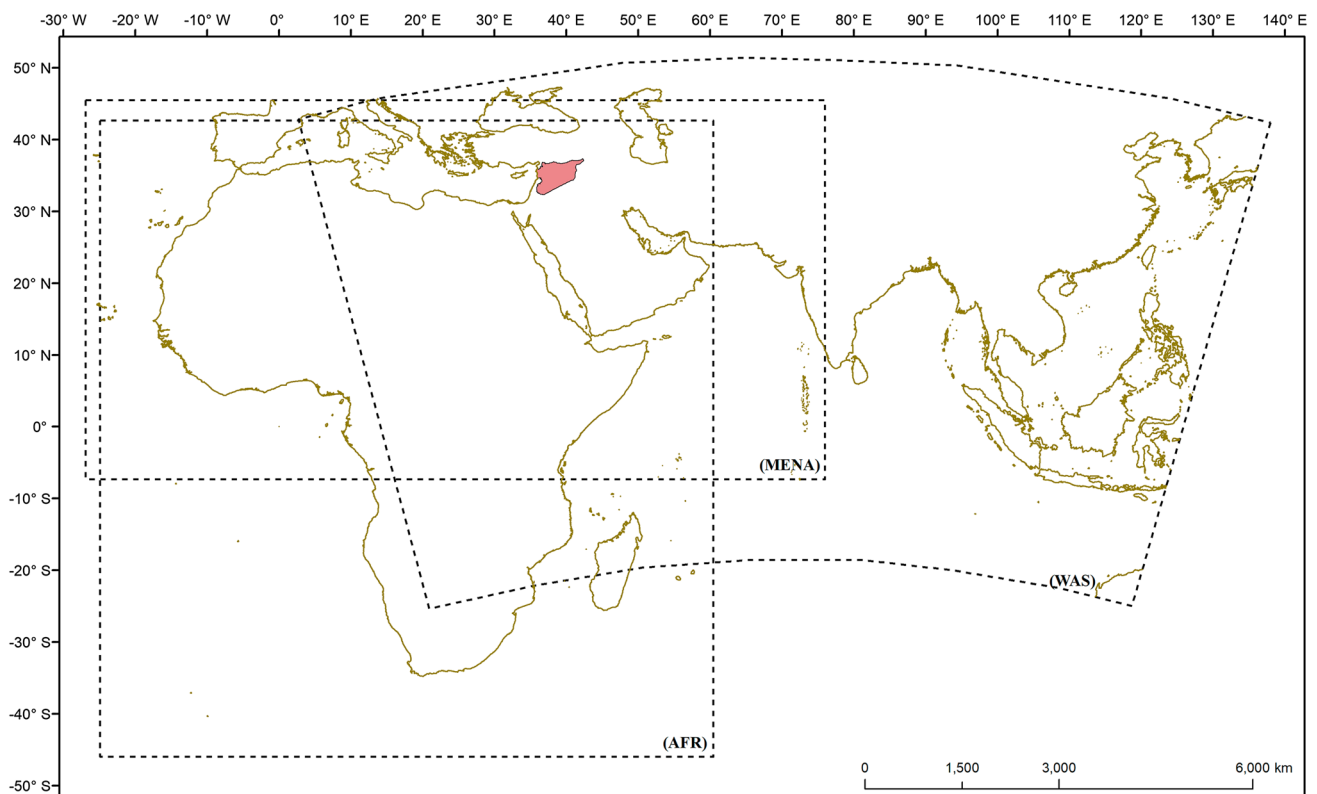


Fig. 1 Location of Syria (highlighted with pink color) within three Cordex domains used in this study

Syria's is characterised by hot, dry and sunny summers (June to August) throughout the country (higher humidity in the coastal areas) and mild, rainy winters (December to February) along the coasts (with occasional snowfall on the highest mountain peaks) (Faour et al. 2010). Details of the observed seasonal mean temperature and precipitation averaged over Syria for the period of 1991–2020 are given in Table 1 (CCKP 2021).

3 Data and Methodology

3.1 Regional Climate Models Description

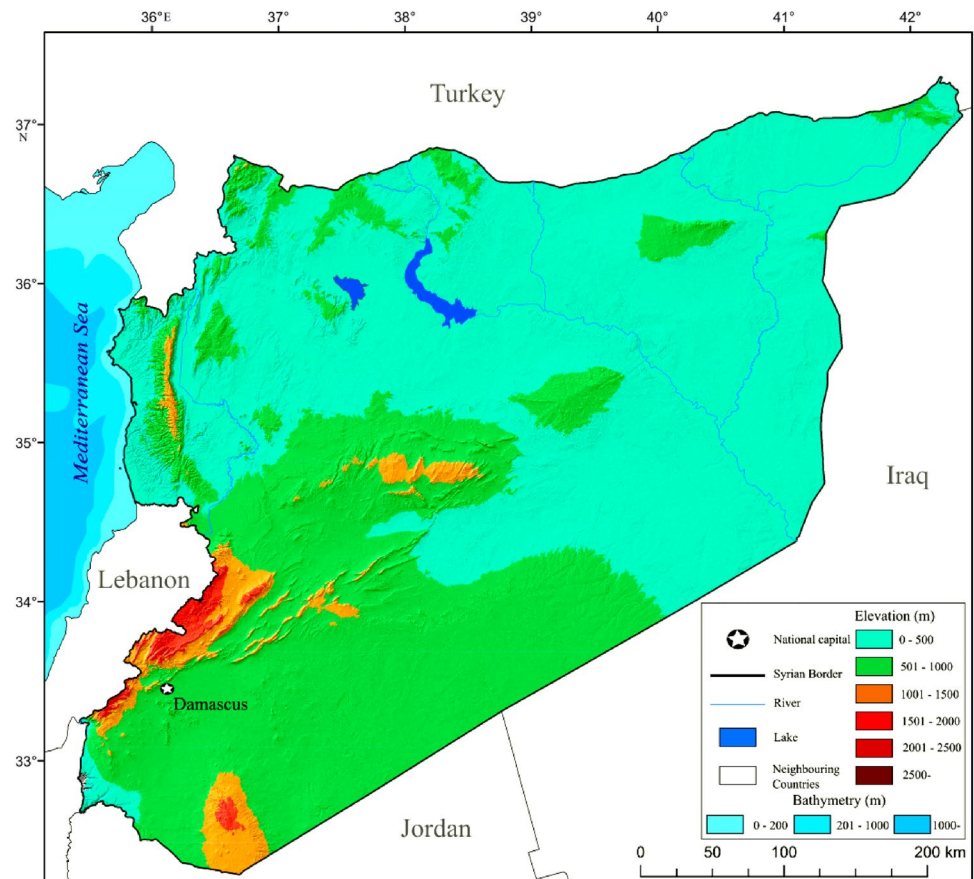
In this section, we provide a brief overview of the models used for simulations conducted over three different CORDEX domains, noting that each domain includes the territory of Syria (Fig. 1). Information on the observational data sets and methods used is also provided in this section.

The CORDEX (Coordinated Regional Climate Downscaling Experiment, <http://wcrp-cordex.ipsl.jussieu.fr/>, Giorgi et al. 2009)—the internationally coordinated initiative was established to provide a relatively high horizontal resolution ensemble of RCM projections over multiple

continental-scale domains for application to climate change impact studies (Gutowski et al. 2016).

Within CORDEX, there are many RCM simulations available for which the initial and boundary conditions are provided by Global Climate Models (GCMs). Such experiments can serve as projections of how the Earth's climate may change in the future. Note that additional simulations are available within CORDEX that are forced by reanalysis fields (representing the perfect boundary condition simulations; Giorgi 2019). These results can also help decision-makers to formulate relevant policies in the context of climate change. However, the impacts of a changing climate and the adaptation strategies need to be considered on both regional (national) and global scales. This is where regional downscaling techniques play an important role, as they provide much more detailed projections and a more accurate representation of extreme events even at the local level compared to GCMs (Wang et al. 2015; Torma et al. 2015; Ciarlo et al. 2021).

In this context, the present study provides an analysis of the CORDEX regional climate model simulations of different climatological variables over Syria (temperature, precipitation, solar radiation and cloud cover). It also provides a brief summary of the expected changes in climatic

Fig. 2 Topography (m) of Syria**Table 1** Observed temperature and precipitation seasonal means for Syria

	DJF	MAM	JJA	SON
Temperature (°C)	7.88	17.58	29.01	20.21
Precipitation (mm)	104.98	84.61	2.85	50.57

conditions for the near (mid) and for far future (end of the twenty-first century) over the region of interest.

The RCMs have the same spatial resolution over each domain (0.44° , ~ 50 km grid spacing). However, in this study we have analysed three time slices: 1989–2008, considered as the present climate (or evaluation period). These 20 years were chosen based on the availability of the evaluation data for both RCMs and observations (Table 2). 1989–2008 also served as the reference period. Historical simulation data used in climate change assessments, which also used data from the scenario runs for 2031–2050 (near future) and 2080–2099 (far future) under the intermediate RCP4.5 and the high-end RCP8.5 scenarios (Moss et al. 2010).

The RCM projections used in this study cover the period 2006–2100, whereas the historical runs cover the period 1970–2005. Accordingly, the driving fields for the scenario runs were provided by GCMs from the CMIP5 experiment

(Climate Model Intercomparison Project, Phase 5; Taylor et al. 2012). RCM simulations for which the lateral boundary conditions were obtained from global reanalyses of observations (perfect boundary condition approach; Giorgi 2019) were also used for the present study. These evaluation runs cover the period 1989–2008. Considering the availability of observational data and RCM data for each variable, the last 3-year period for present climate data was provided by the RCP8.5 scenario runs for the RCMs.

Details of the CORDEX RCMs and their driving fields used in the study are shown in Table 2. We analysed these simulations conducted at different model centers. It should be noted that the evaluation simulations cover different time slices, making it difficult to obtain 30 consecutive years.

3.2 Observational Data

Noting that, not only observational data sets can serve as reference data for validation purposes, but reanalysis data can also be used to evaluate the performance of climate model simulations (Zhang et al. 2011; Moalafhi et al. 2017; Eadain et al. 2021). Thus, reanalysis data sets can be used as an alternative solution when there is a gap in observational data over the study area.

Table 2 CORDEX–RCMs and the driving fields used in this study

RCM	Model centre	Driving field	Region	Evaluation runs availability		
				Start	End	Count (years)
HIRHAM5 Christensen et al. (1998)	Danmarks Meteorologiske Institut (DMI), Danmark	ECMWF–ERAINT ICHEC	AFR	1989	2010	22
RACMO22T Meijgaard et al. (2012)	Koninklijk Nederlands Meteorologisch Instituut (KNMI),	ECMWF–ERAINT ICHEC MOHC	AFR	1981	2010	30
REMO2009 Jacob (2001)	Climate Service Center Germany (GERICS)	ECMWF–ERAINT ICHEC IPSL MIROC MOHC MPI	AFR	1989	2008	20
RCA4 Kupiainen et al. (2011)	Sveriges Meteorologiska och Hydrologiska Institut (SMHI), Sweden	ECMWF–ERAINT CNRM ICHEC NOAA	MNA	1981	2010	30
RegCM4 Giorgi et al. (2012)	National Center for Atmospheric Research (NCAR) and Earth System Physics (ESP)	ECMWF–ERAINT CNRM CSIRO IPSL MPI NOAA	WAS	1981	2008	28

As reference data for validation purposes, we used different types of data sets, namely: land surface station measurement data (CRU, Climatic Research Unit, Harris et al. 2020), reanalysis product (ERA5, Hersbach et al. 2019), and satellite-based observations (SARAH-2; Pfeifroth et al. 2018).

CRU is a widely used climate data set covering all land areas of the world except Antarctica, with observations dating back to 1901. It is derived by interpolating monthly climate anomalies from extensive networks of weather station observations (Harris et al. 2020). The data set used in this study is version 4.04, which contains three different climate variables: temperature (tmp), precipitation (pre) and cloud cover (cld).

At the same time, the ERA5 reanalysis data set (Simmons et al. 2006) has several advances (including better spatial and temporal resolution) compared to ERA-Interim (Hoffmann et al. 2019) and is based on the Integrated Forecasting System (Hersbach et al. 2019). It combines large amounts of historical observations into global estimates using advanced modelling and data assimilation systems that provide data from 1950 onwards (the research uses a reanalysis data set with a publication date of 2019-04-18, including three different climate variables: solar radiation, precipitation and temperature).

The second edition of the Surface Solar Radiation Data Set–Heliosat Edition 2 (SARAH-2; Pfeifroth et al. 2018) is

used for further model evaluation, and CLARA-A2 from EUMETSAT CM-SAF (Karlsson et al. 2020) is used.

E-OBS v23.1e (Cornes et al. 2018) is also used as an additional observational reference data set. This observational gridded data set covers the region of interest; however, it mostly consists of station data from Europe with a horizontal resolution of $0.1^\circ \times 0.1^\circ$ and $0.25^\circ \times 0.25^\circ$. The obtained version of E-OBS contains eight meteorological variables on a daily basis from 1950 to 2020. For our purpose, to validate the RCM simulations, tg, rr and qq fields were obtained from the E-OBS data set at a resolution of $0.25^\circ \times 0.25^\circ$.

3.3 Methodology and Analyses

The metrics used for the present study are commonly used by the CORDEX community for both assessment and climate change studies (Kotlarski et al. 2014; Gutowski et al. 2016; Giorgi 2019). Our analysis has two main focuses. First, we evaluated the performance of the RCMs in reproducing the present-day climate during the period of: 1989–2008, focusing on some key meteorological variables: cloud cover (clt), solar irradiance (rsds), near surface temperature (tas) and total precipitation (pr). More specifically, the simulated climate variables over Syria were compared with observations obtained for the present climate (1989–2008) from the

following data sets: CRU (clt, tas and pr), CLARA (clt), SARA (rsds) and ERA5 (rsds, tas, pr). Accordingly, all RCM and observational data were interpolated to share the same horizontal grid by following previous work (Torma et al. 2015). The interpolation technique used was the distance weighted average remapping of the Climate Data Operators software (CDO, Sczhuizweida, 2021). All data are then analysed and reported on the common 0.44° km grid. Annual cycles are calculated on a monthly basis, averaged over the region of interest (Fig. 2).

The biases present in the simulated climate variables were calculated with respect to the observations: model minus observation. In this form, a positive bias in precipitation refers to its overestimation, while a positive bias in temperature indicates warmer conditions in the model compared to observations.

Accordingly, the spatial distribution of simulated and observed data over Syria was also compared. The normalised standard deviation and spatial correlations were calculated and compared with the observational data and represented in the form of a Taylor diagram (Taylor 2001). Calculations were performed on a seasonal scale representing four seasons: winter (December–January–February, DJF), spring (March–April–May, MAM), summer (June–July–August, JJA) and autumn (September–October–November, SON) and all RCMs and other additional observational data sets were compared to a reference data set: CRU.

We then turned our attention to the projected changes relative to the reference period for the following two scenarios: RCP4.5 and RCP8.5 and two time slices near future (2031–2050) and far future (2070–2099). The projected changes are presented in the form of spatial plots with respect to the reference period 1989–2008. Based on the spatial means of the projected temperatures, the expected rate of temperature change is also given for the region of Syria.

4 Results and Discussion

4.1 Present Climate (Annual Means)

We first evaluated the performance of five RCMs (five evaluation experiments) in reproducing 20 years of annual means (1989–2008) with respect to two observational data sets for each variable (Fig. 3).

The ensemble means capture the general pattern of the observations very well and reproduce the observed spatial distribution of all analysed variables (rsds, clt, tas and pr); however, a slight difference is present in reproducing cloud cover and radiation. In general, the simulations show a precipitation gradient from west to east (the more humid western coastal areas compared to the dry areas in the east, leading to local precipitation minima over the southeastern

region of Syria). Similarly, the temperature also shows the aforementioned west-to-east gradient (near the coast, the air contains more water vapour, resulting in higher humidity with a chance of fog formation over western coastal areas and higher inland areas). If the air mass comes from the sea, the relative humidity will be high, bringing cooler air to the western parts compared to the eastern ones.

Solar radiation shows a solid strong north–south gradient with a maximum of 245 W/m² per month in the southern parts in the observations, a pattern generally reproduced by the RCMs, but with a slight underestimation.

The spatial distributions of the simulated and observed meteorological variables over Syria also show a strong correlation between the four variables, as areas with lower (higher) temperature and solar radiation values are associated with higher (lower) cloud cover and precipitation values (Fig. 3). In addition, we can also see the clear signal of the effect of the high altitude areas (over 1000 m above sea level) located mainly in the western parts of the region, which is manifested in the local minimum of temperature and local maximum of precipitation and cloud cover.

Overall, the ensemble mean of the five RCMs shows a relatively good ability to reproduce most of the observed climatology and to capture the general pattern of the observed data. In addition, our results also highlight the fact that there are uncertainties in the observational data. For example, we used two different observational data sets for each meteorological variable assessed to draw attention to this fact. In general, the CRU data set was used as the reference database, except for the radiation (rsds), as such a variable is not provided by CRU, thus we used SARA as the reference data set.

4.2 Temperature and Precipitation Biases for the Present Climate (Seasonal Means)

The differences between the RCMs (evaluation runs for which ERA-Interim provided the forcing fields) and the observed climatology are shown in Figs. 4 and 5. More specifically, these biases are calculated by computing the differences between model and observed data (model minus observation), where a positive bias indicates overestimation of a given variable by the RCM, while a negative bias reflects an underestimation of that variable relative to observations.

4.2.1 Temperature

In general, the RCMs tend to be warmer over the south-western regions and cooler in the northernmost areas than the observations, with the CRU serving as the reference data set.

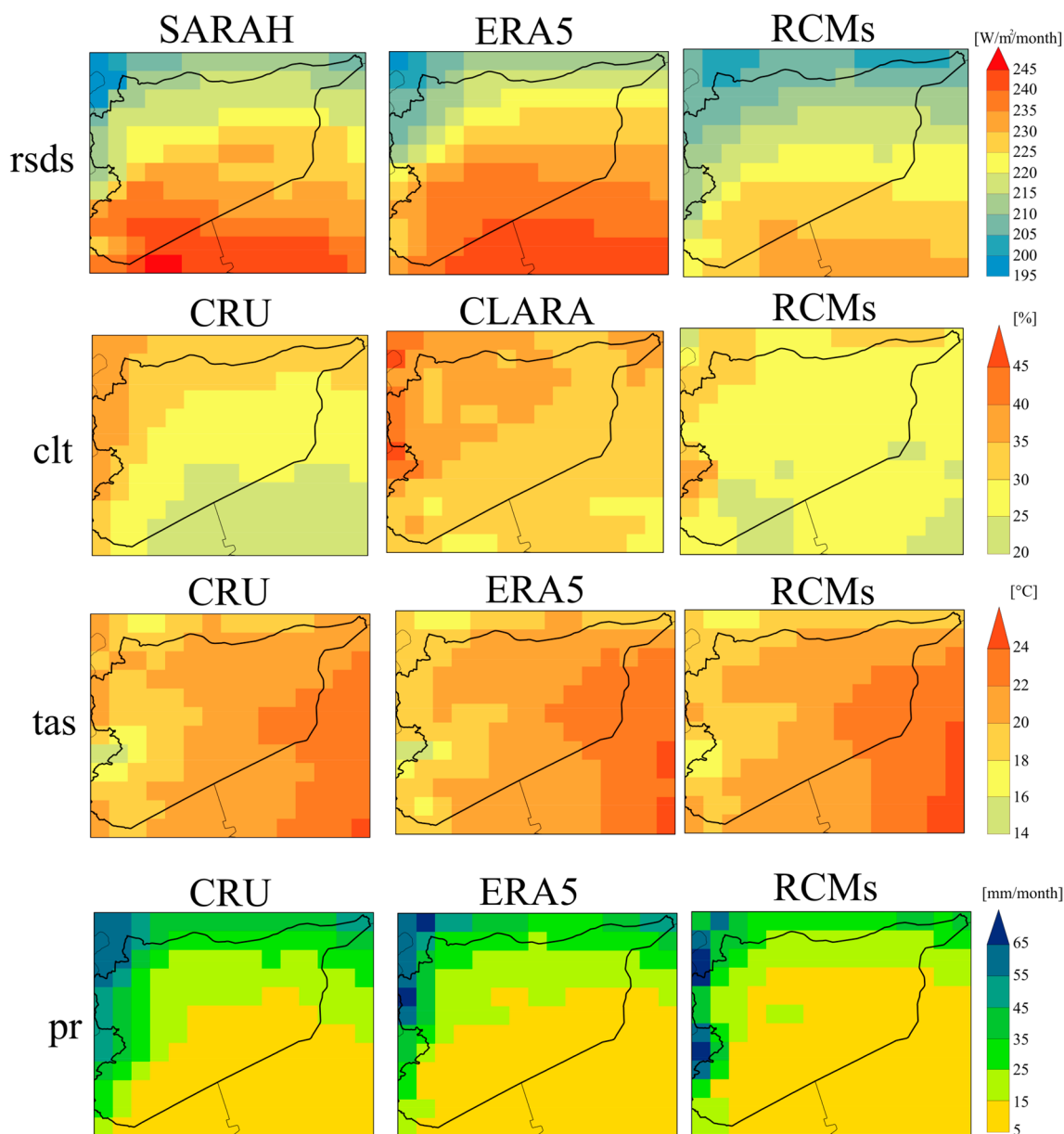


Fig. 3 20-year annual mean of solar irradiance (rsds), total cloud cover (clt), air temperature (tas) and precipitation (pr) of the period between 1989 to 2008

RCA4 was found to be an outlier in terms of spatial biases in terms of magnitude. RCA4 strongly underestimates the seasonal temperature in all seasons, except for SON.

REMO and HIRHAM were found to be among the best performing RCMs for winter mean temperature, while RACMO was best at simulating the temperature characteristics in other seasons. For example, RACMO showed relatively small biases over the Syrian region compared to the other RCMs.

Four RCMs (RegCM, HIRHAM, RACMO and REMO) overestimated temperature in most grids within the range of absolute biases of ± 3 °C.

4.2.2 Precipitation

Similar to temperature, the validation is carried out by comparing the individual evaluation RCM simulations with the CRU data set (Fig. 5). The region of interest is characterised by low annual precipitation totals (see Sect. 2), so small biases can lead to large relative biases. For this reason, the biases shown here are expressed in mm/month rather than in %. However, the field means of these bias fields are also given in % in Table 3 in Sect. 4.3.

Seasonal precipitation fields are typically underestimated by all RCMs compared to observations, with an absolute

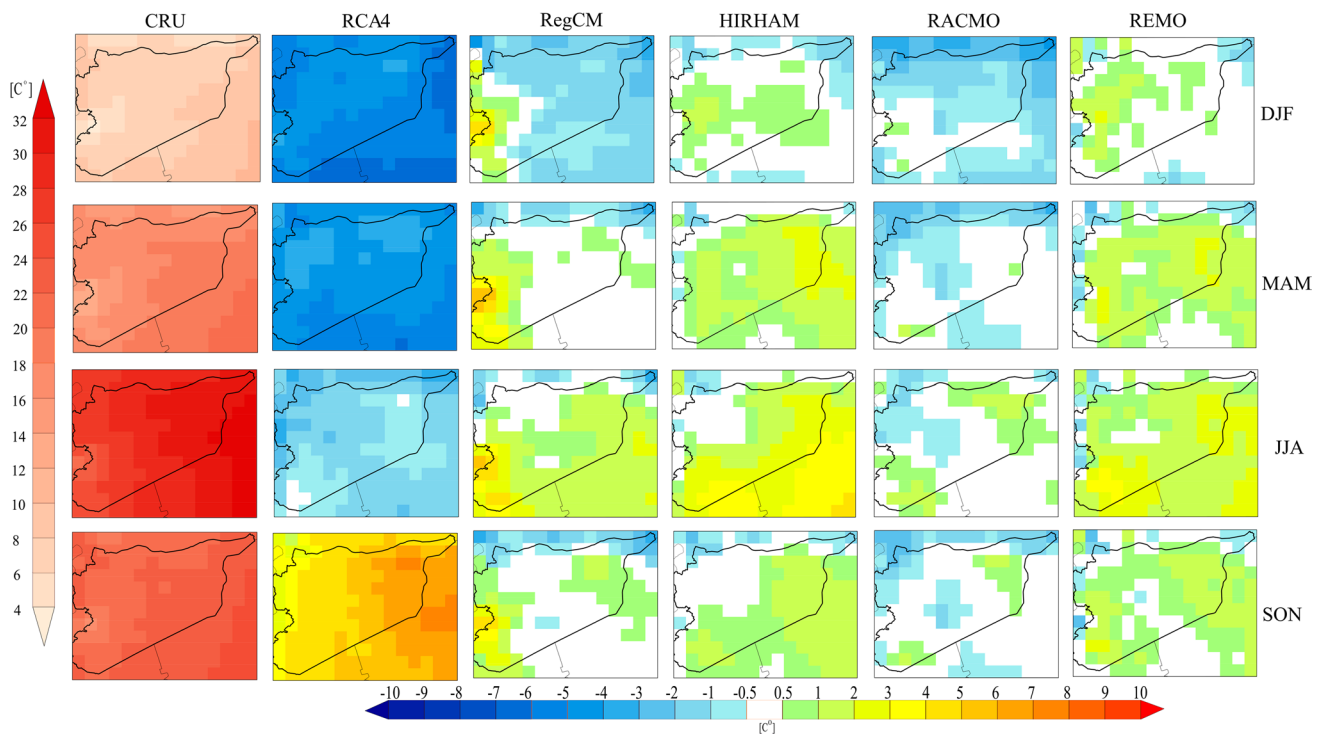


Fig. 4 Mean seasonal surface temperature ($^{\circ}\text{C}$) biases (1989–2008) for all RCM experiments for December–February (DJF, first row), March–May (MAM, second row), June–August (JJA, third row) and

September–November (SON, fourth row) compared to CRU. The first panel of each row shows the spatial pattern of seasonal mean temperature as provided by the CRU reference data set ($^{\circ}\text{C}$)

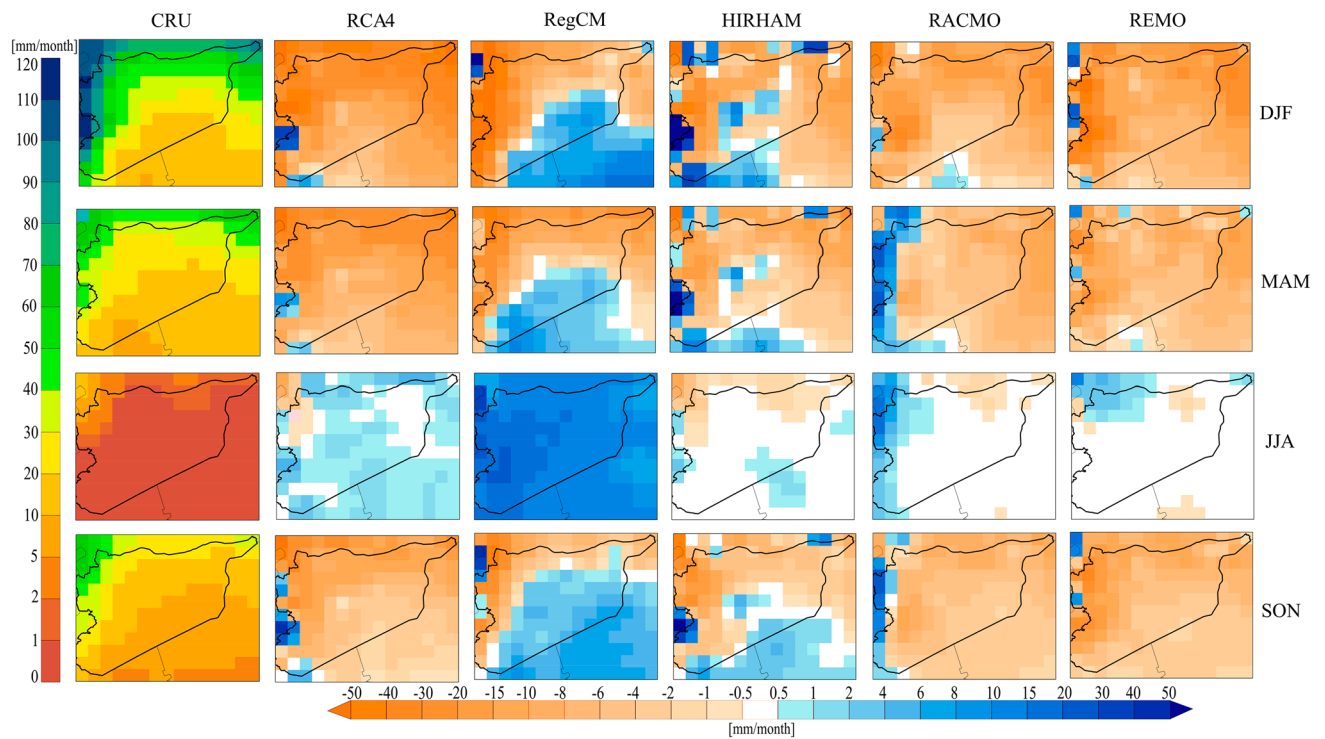


Fig. 5 As shown in Fig. 4, but for precipitation (mm/month)

Table 3 Seasonal temperature, precipitation, solar radiation and cloud cover biases averaged over the region of interest (compared to the reference data set (CRU) for temperature, precipitation and cloud cover and (SARA) for solar radiation)

	RCA4	RegCM	HIRHAM	RACMO	REMO
Temperature (°C)					
DJF	- 1.21	- 0.9	0.07	- 1.18	0.21
MAM	1.12	0.34	1.01	- 0.57	0.76
JJA	1.58	1.12	1.82	0.12	1.39
SON	- 0.39	0.2	0.65	- 0.32	0.59
Precipitation (%)					
DJF	- 47.68	- 20.1	- 5.31	- 23.7	- 31.98
MAM	- 51.94	- 18.86	- 9.62	- 12.6	- 21.89
JJA	117.42	2467.93	- 44.86	108.34	43.31
SON	- 13.27	183.87	- 7.8	18.67	- 20.26
Solar radiation (%)					
DJF	18.59	3.99	- 19.91	9.19	- 16.07
MAM	12.16	4.64	- 9.55	4.97	- 10.33
JJA	- 1.61	- 6.87	- 8.94	- 6.32	- 7.4
SON	6.27	5.4	- 17.72	- 0.61	- 14.43
Cloud cover (%)					
DJF	- 28.25	- 6.12	4.06	- 6.55	- 15.99
MAM	- 26.56	- 9.18	1.68	- 11.82	- 14.45
JJA	32.43	520.01	- 9.68	- 33.5	- 33.01
SON	- 4.91	93.07	57.58	- 5.37	- 16.28

bias in the range of ± 50 mm/month. All RCMs have a strong dry bias all over most of the study area, except RegCM, which has a wet bias is present over the southern regions regardless of the season. RegCM also has a strong wet bias over every grid cell in JJA, which can be attributed to the sensitivity of the convective parameterisation scheme used by the model.

In general, the evaluation of the climate models in terms of the biases showed that most RCMs had a dominant dry bias (underestimation of precipitation) in most of the region of interest in all seasons, except for JJA. The smallest biases were found for JJA, except for the RegCM (note that the mean seasonal precipitation is lowest in summer, see Sect. 4.3 for more details).

Figure 6 shows the Taylor diagrams based on the seasonal means of additional observational data sets and also including RCMs averaged over the reference period: 1989–2008.

A total of 22 simulations are shown in Fig. 6 (including five evaluation and five historical runs, see Table 2). In general, the RCMs have similar skills to represent the present climate, regardless of the simulation (evaluation or historical run). However, there are differences between the RCMs for some variables and in the different seasons.

For example, in terms of representing the seasonal characteristics of temperature (tas) and solar radiation (rsds), the RegCM simulations (purple colour) represent close to 1

normalised standard deviation (STDV, which indicates that the pattern variations are of the right amplitude compared to the observations) in all seasons, but are associated with relatively low spatial correlation.

The largest differences were found for the variables cloud cover (clt) and precipitation (pr). These variables show higher variability in space and time compared to temperature and radiation, thus challenging climate models. However, for JJA the HIRHAM simulation is close to the observed precipitation data, with the highest correlation coefficient (0.9).

The symbols representing RegCM for summer cloud cover data are not shown in Fig. 6. This also indicates that RegCM is an outlier compared to other RCMs.

The analysis of Fig. 6 also shows that the performance of the RCMs is seasonally and variable dependent: the best results for the given metrics were found for temperature for JJA, not for precipitation. Overall, considering all variables and seasons, REMO and RACMO were found to be the best performing RCMs over the region of interest.

4.3 Annual Cycle

Figure 7 shows the annual cycle based on the monthly means for the four analysed variables averaged over the region of interest. It can be seen that for temperature and solar radiation, most of the 22 models evaluated (five evaluation and seventeen historical) capture the annual cycles very well, and all the RCMs analyse are in agreement. Some models could be an exception, HIRHAM, and REMO (e.g., rsds).

When looking at the annual cycles of precipitation and cloud cover, most models (except for RegCM) seem to underestimate the observations, especially during the winter season.

RegCM could not capture the annual cycle for clt and pr. It seems that the parameterisation of the RegCM for this region is too sensitive to convection, leading to relatively high summer precipitation (see also Fig. 5). Therefore, further tuning of this RCM is needed to find the optimal parameterisation setting for the Syrian region.

In summary, the majority of the models seem to capture the annual cycle [especially the peak in the summer months (tas, rsds) and the decline in the winter months (pr, clt)]. It should be noted that no single model performs best in representing all the variables, which also highlights the need for the ensemble technique. Furthermore, the results reported in Fig. 7 also highlight the uncertainties associated with RCM simulations (Giorgi and Bi 2000; Deque et al. 2007; Giorgi 2019).

The seasonal spatial means of the biases reported in Fig. 7 are given in Table 3. It can be seen that the above mentioned biases are more pronounced in the case of precipitation and cloud cover for RegCM. More specifically, in the case of summer precipitation (when precipitation in

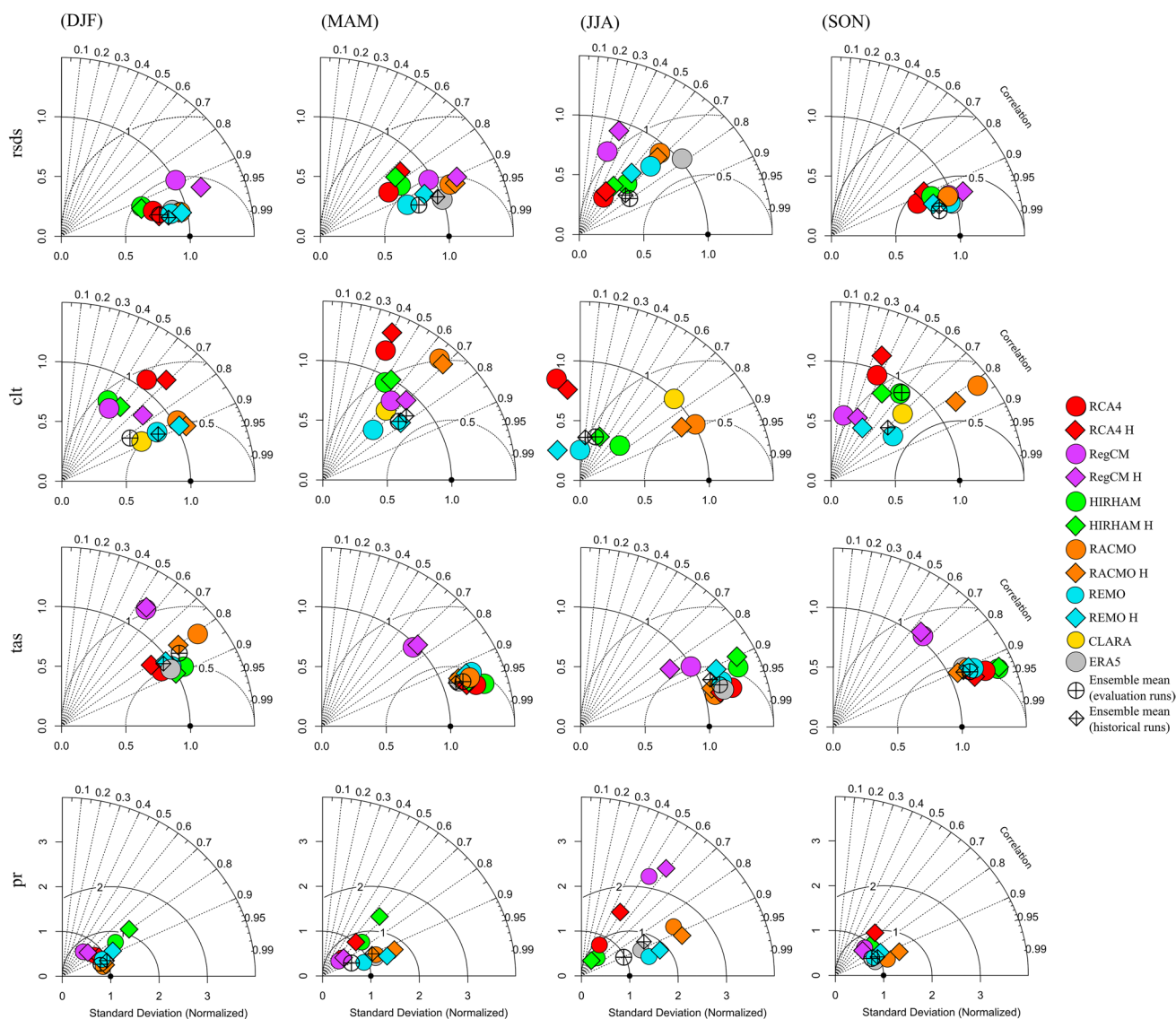


Fig. 6 Taylor diagram of mean (1989–2008) seasonal radiation (rsds, first row) vs. SARA, cloud cover (clt, second row), temperature (tas, third row) and precipitation (pr, fourth row) vs. CRU. The four col-

umns are for the four seasons (RCM names refer to the evaluation runs, while ‘H’ refers to the historical simulation mean of each RCM group.)

general shows high variability in space and time), the results can be sensitive to the choice of parameterisation used for convective processes.

4.4 Future Climate, Projected Changes in Climate Variables

After evaluation of all the RCMs mentioned, and as a result of the assessment, only four RCMs were selected for the climate change assessments (Table 4). The decision was based on all previous bias assessments as well as data availability (the selected simulations must also share the same time period for each emission scenario and only one selected run per RCM was chosen to avoid the results of a given RCM

dominating the ensemble mean). Finally, we excluded the RegCM from the assessment of the future scenario runs because of its opposite behaviour compared to other RCMs (e.g., Fig. 7) and the high biases that the RegCM generally represents over the region of interest (Figs. 5 and 6).

4.4.1 Cloud Cover

Figure 8 shows the projected seasonal changes (relative to the reference period (1989–2008) derived from each historical simulation) in cloud cover under the RCP4.5 and RCP8.5 emissions scenarios for the mid-century (2031–2050) and the end-century (2080–2099). Regions with dots depict robust signals (where 3 out of 4 RCMs agree on the sign of

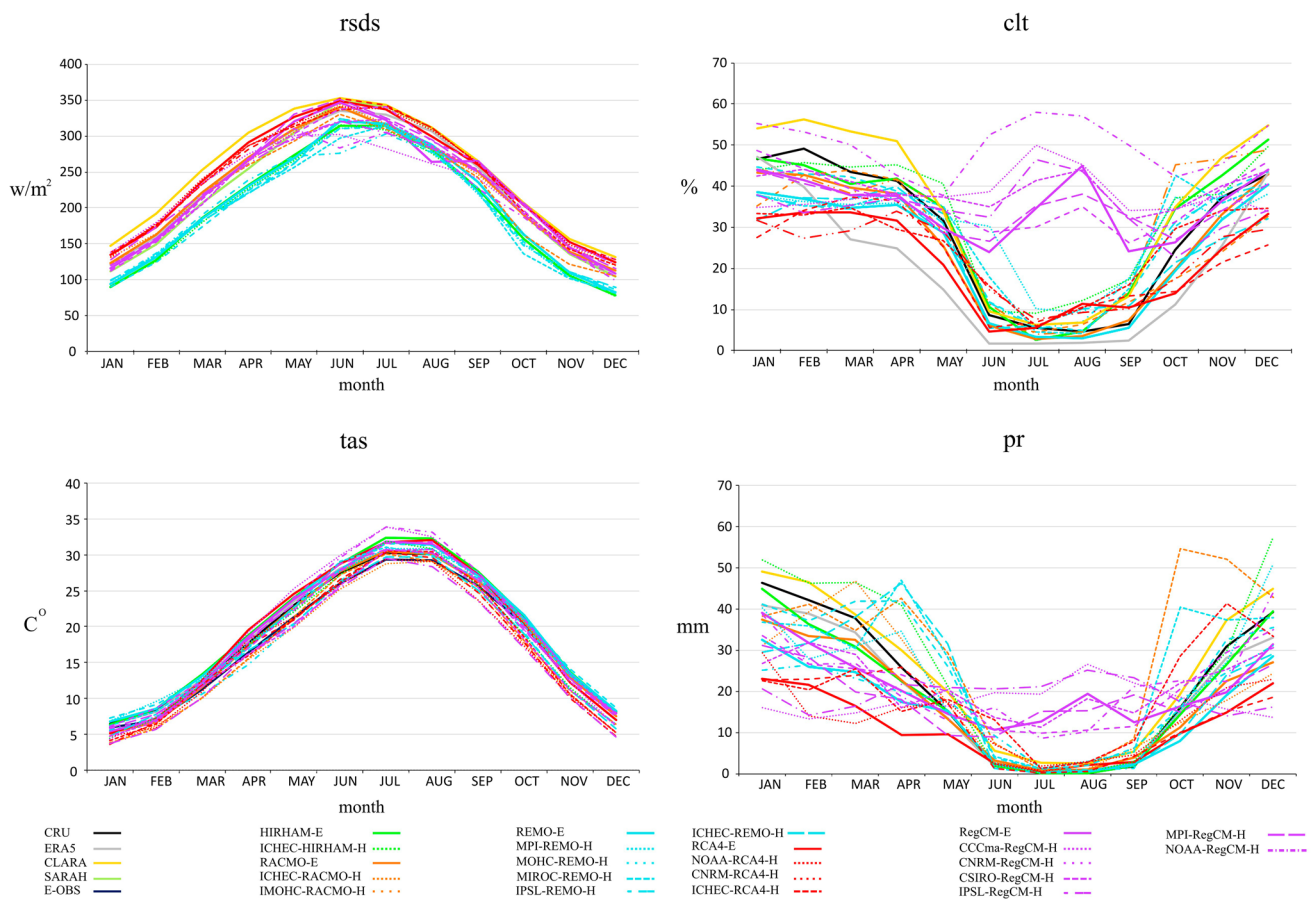


Fig. 7 Annual cycle of the four meteorological variables based on their monthly means averaged over the entire region of Fig. 1 for the period 1989–2008. Noting that, ‘-E’ refer to the evaluation runs, while ‘-H’ refers to the historical simulation

Table 4 CORDEX scenario runs and their availability for climate change assessments

RCM	Region	Model center	Reason to choose/exclude
RCA4	MNA	ICHEC-EC-EARTH	RCP4.5 not available
	MNA	NOAA-GFDL-GFDL-ESM2M	Best performance
	MNA	CNRM-CERFACS-CNRM-CM5	–
HIRHAM5	AFR	DMI-ICHEC-EC-EARTH	Best performance
	RACMO22T	MOHC-HadGEM2-ES	Best performance
REMO2009	AFR	ICHEC-EC-EARTH	–
	AFR	ECMWF-ERAINT	RCP4.5, RCP8.5 not available
	AFR	MPI-M-MPI-ESM-LR	Best performance
	AFR	MIROC-MIROC5	RCP4.5 not available
	AFR	IPSL-IPSL-CM5A-LR	RCP4.5 not available
	AFR	ICHEC-EC-EARTH	–
	AFR	MOHC-HadGEM2-ES	RCP4.5 not available
	AFR	NOAA-GFDL-GFDL-ESM2G	RCP4.5, RCP8.5 not available

Simulations available under both scenarios and selected for further assessment are highlighted in bold

the projected change). Robust signals were also found for the other three variables (see Figs. 9, 10, 11), which may be related to the fact that Syria’s climate will be mainly characterised by a mixture of arid and semi-arid climates.

The general trend is a decreasing fraction of cloud cover throughout the twenty-first century in both RCP scenarios for the region of Syria, which is justified by all models (they all agree on the sign of the change).

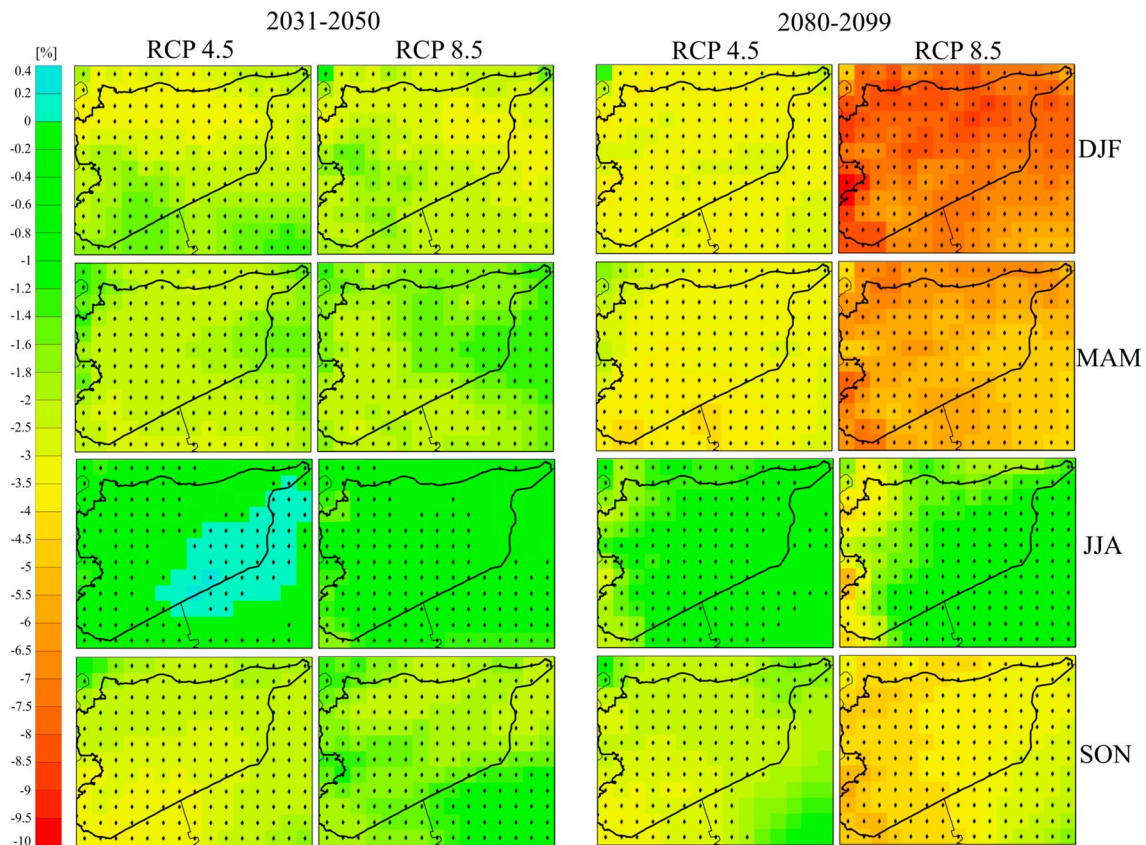


Fig. 8 Projected changes (relative to the 1989–2008 reference period) in mean seasonal cloud cover under RCP4.5 and RCP8.5 scenarios. Units are in %

The most pronounced changes corresponding to the RCP8.5 scenario are found for the winter and spring seasons. According to our results, the population of Syria will face a higher decrease in the percentage of cloud cover (between 6% and 10%). More specifically, the coastal areas located in the western parts of Syria seem to be the areas most affected by this change. However, the only exception to this behaviour is during the summer season under RCP4.5 (terquaz colour), where there could be a relatively small increase in the eastern part of Syria during the summer of the mid-century period (Fig. 8).

The decrease is present in all seasons. In the summer season, when there is not a high percentage of cloud cover, the coastal areas still show the greatest decrease. All in all, this could lead to more intense evaporation, which could make the region drier in the coming decades.

Global warming will affect the Syrian coastal areas of the Mediterranean Sea mainly through changes in the hydrological cycle, with less moisture being transported from the tropics towards the poles. The resulting decrease in precipitation over the coastal basin could also lead to a substantial decrease in the river runoff.

4.4.2 Precipitation

Similar to the projection of cloud cover change, the results are also reflected in the decrease of precipitation over the study area (Fig. 9).

The change under RCP8.5 is generally more pronounced than under RCP4.5 by the end of the twenty-first century. However, by mid-century, the RCMs show a greater decrease in precipitation under RCP4.5 compared to RCP8.5, especially for the eastern parts of the region.

Overall, most RCM simulations show a strong decreasing trend in mean summer precipitation, regardless of the forcing scenario. Some seasonal dependencies were also found: the most pronounced changes in terms of decreasing seasonal precipitation totals are expected for JJA and MAM, while less pronounced or even weak precipitation increases are found for DJF and SON. Our results also draw attention to the fact, that the assessed RCM simulations project a typically drier climate over the region of interest by the end of the twenty-first century.

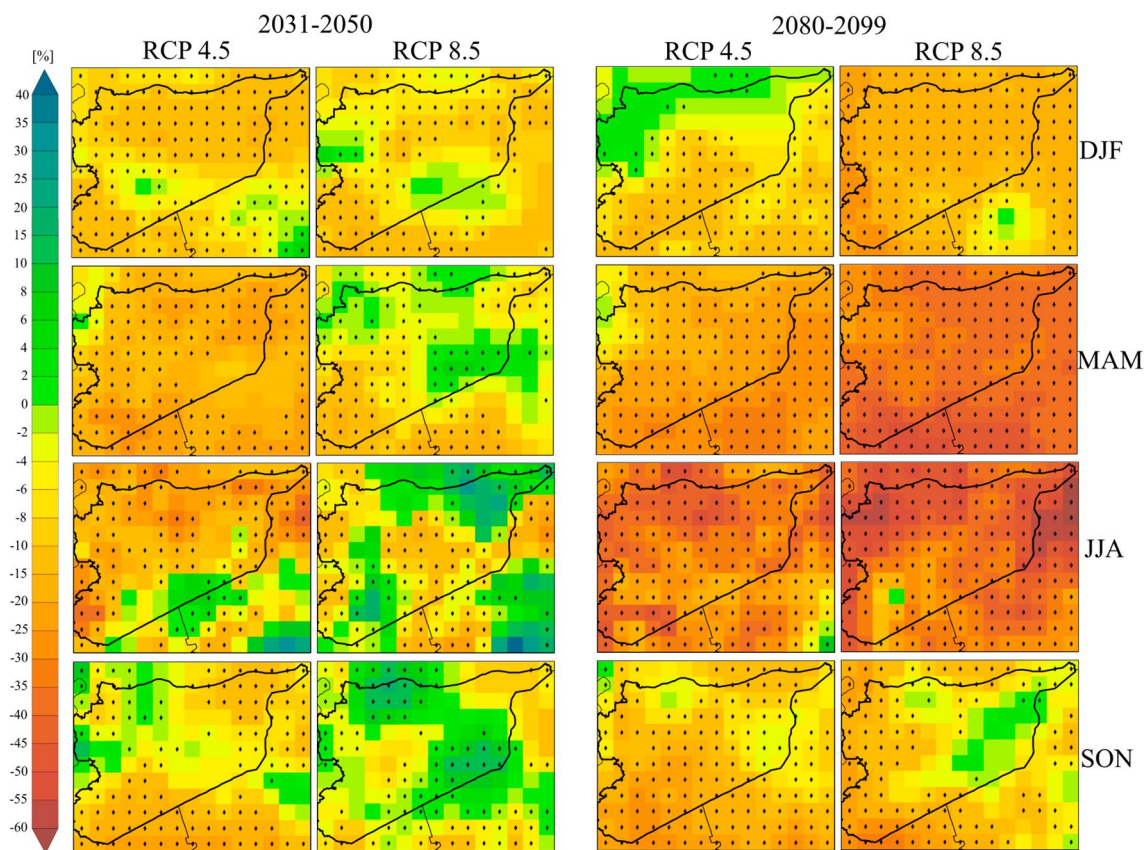


Fig. 9 Same as Fig. 8, but for precipitation

The detailed description of the uncertainty associated with the projected annual mean precipitation for Syria under the two future scenarios is provided in Table 5, Sect. 4.4.4.

4.4.3 Solar Radiation

Figure 10 shows the expected change in solar radiation and the ensemble mean of the four selected RCMs under the moderate and high-end scenarios.

Looking at the general pattern of change in both scenarios, two different behaviours can be observed: in winter and spring (increase), but for summer and autumn the results are mixed: between positive signals (over some part of the study region in SON) and a dominant decrease (over most of Syria in JJA). All these changes are projected for both future periods (2031–2050 and 2080–2099).

The largest decrease in solar radiation under both scenarios is projected during the autumn season (SON) and is located in the south-eastern part of the region. We also found this signal to be robust, as most RCMs show strong agreement on the sign of this change. Furthermore, the expected maximum increase in seasonal solar irradiance coincides with the projected maximum decrease in cloud cover under RCP8.5 (Fig. 8).

Based on this, it has been shown that future changes in solar energy potential are sensitive to the level of global warming that is projected to occur by the end of the twenty-first century under different emission scenarios.

The relationship between temperature and solar radiation has a notable effect, as the greater the increase in near-surface temperature, the greater the potential for future solar energy suitability, and the projected changes in solar radiation more or less support the direction of changes in the photovoltaic potential (Dutta et al. 2022). In this respect, this study provides an important scientific reference to support the benefits of mitigation and the feasibility of large-scale deployment of solar power in a changing climate.

Changes in the amount of solar radiation (increasing trend over western and northern parts of Syria) may not have a negative impact on households if the region is open to solar energy generation. On the contrary, some regions can be expected to benefit from an increase in solar energy.

4.4.4 Temperature

Based on the results of the assessed RCM simulations, Syria will be a region strongly affected by global warming (Fig. 11). The temperature change is considered robust over

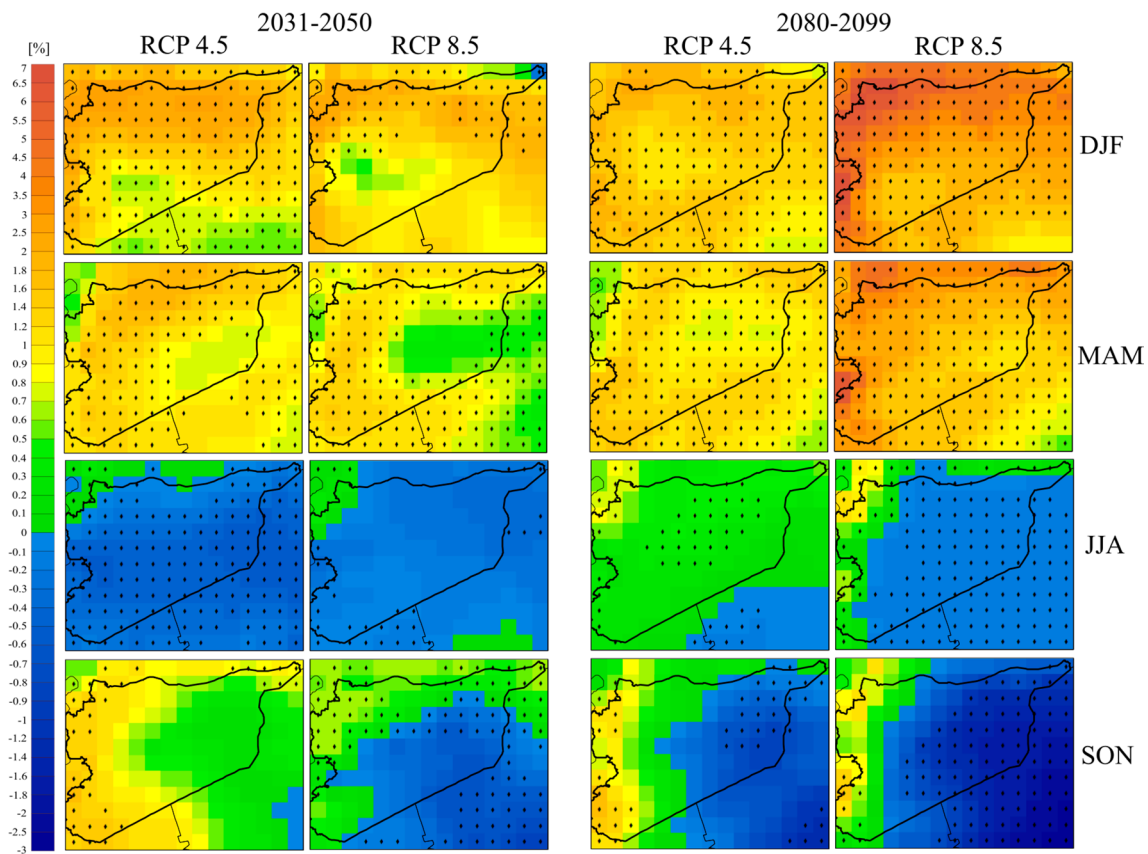


Fig. 10 Same as Fig. 8, but for solar radiation

all grid points in all seasons and under both scenarios, thus no additional points are overlaid on sub-panels in Fig. 11.

Irrespective of the season, all RCMs show substantial temperature increases, especially over the eastern parts of the region. The maximum temperature change is expected in summer (1.8 °C, the highest under RCP4.5 and could reach 6 °C under RCP8.5).

These temperature increases, combined with the projected decrease in precipitation (Fig. 9), raise the issue of meteorological droughts under both climate scenarios. The overall increase in mean temperature is robust in both magnitude and sign over the vast majority of the Syrian territory.

Such an increase in mean seasonal temperatures associated with a decreasing trend in cloud cover and decreasing precipitation totals, is likely to lead to a significant increase in evaporation in coastal regions. A semi-arid country is already suffering from water scarcity, which, combined with a decrease in precipitation, could lead to a shift towards more arid climates.

The seasonal temperature changes shown in Fig. 11 are also evident when we look at the individual projections under the RCP4.5 and RCP8.5 scenarios (Fig. 12). The curves are obtained by taking the difference of each

future year (with respect to the mean of the reference period (1989–2008) derived from each historical simulation) and the shaded areas around each of the curves represent the minimum and maximum changes based on these simulations (Table 5). The temperature change during the twenty-first century is more pronounced under the RCP8.5 scenario than under RCP4.5, and the range of projections increases towards the end of the century (shaded areas in Fig. 12).

Table 5 reports the seasonal uncertainty for temperature (°C) and precipitation (%) for the mid (2031–2050) and far (2080–2099) future periods compared to the reference period (1989–2008) under the two RCP scenarios.

The range of temperature and precipitation changes is larger under the high-emission scenario than in the moderate one. In addition, the range of simulated changes increases towards the end of the twenty-first century (Table 5). The variability of projected temperature changes among the ensemble members is in the range of 0.5–0.9 °C (RCP4.5) and 0.5–1.6 °C (RCP8.5) for the near and far future, respectively. The projected precipitation signals, however, show a much more varied picture (Table 5).

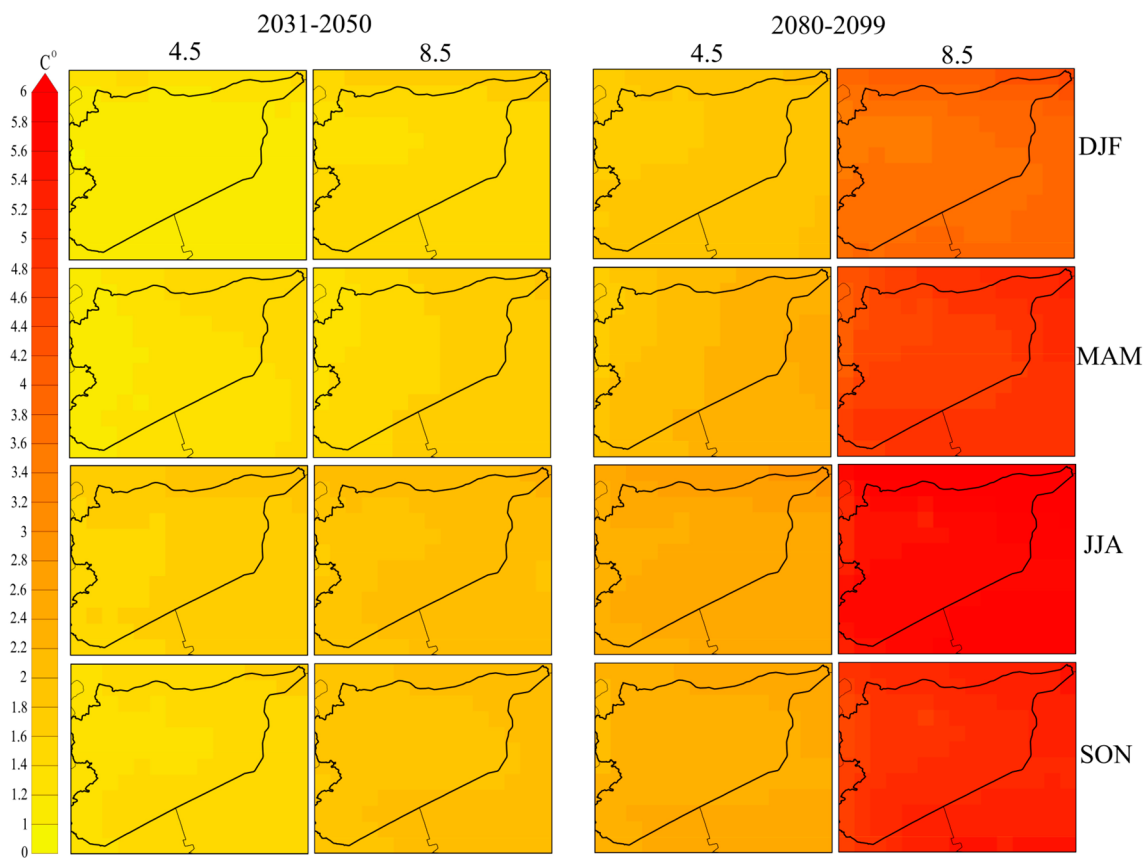


Fig. 11 Same as Fig. 8, but for temperature. Units are in °C

Table 5 Minimum and maximum changes in seasonal mean temperature (°C) and precipitation (%) over Syria relative to the reference period: 1989–2008

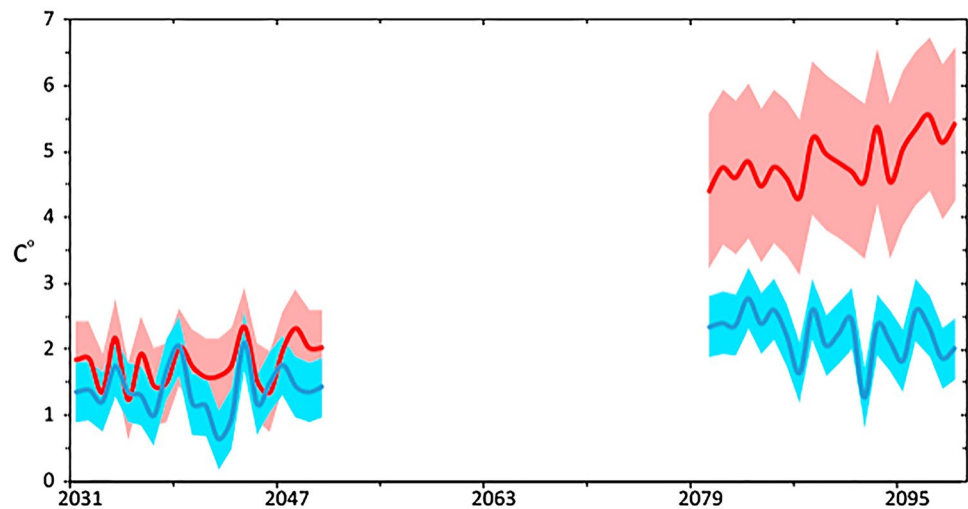
	RCP4.5				RCP8.5			
	Mid (2031–2050)		Far (2080–2099)		Mid (2031–2050)		Far (2080–2099)	
	Min	Max	Min	Max	Min	Max	Min	Max
Temperature (°C)								
DJF	1	1.41	1.62	2.1	1.34	1.8	3.46	4.51
MAM	1.02	1.53	1.68	2.5	1.25	1.83	4.03	5.22
JJA	1.49	1.98	2.21	2.91	1.8	2.24	5.09	6.63
SON	1.26	1.66	2.15	2.52	1.77	2.18	4.55	5.45
Precipitation (%)								
DJF	– 15.49	7.17	– 15.56	3.43	– 16.46	5.58	– 29.8	0.18
MAM	– 29.25	0.28	– 34.73	– 0.88	– 18.5	6.31	– 51.69	– 22.58
JJA	– 40.13	34.4	– 52	9.77	– 26.16	41.26	– 63.71	0.65
SON	– 22.11	10.12	– 29.68	0.6	– 14.16	15.87	– 32.38	3.88

5 Conclusion

This study investigates the climate of Syria and its surroundings using an ensemble of RCM simulations performed over three different CORDEX domains with a horizontal resolution of 0.44° (~ 50 km grid spacing). We

evaluated several metrics related to the performance of RCMs representing the present climate (1989–2008) and validated them against different observational data sets focusing on four climate variables: solar irradiance, cloud cover, air temperature and precipitation. We also turned our attention to the future climate projections, hence the assessment of the twenty-first century projections

Fig. 12 Projected changes in mean annual temperature for Syria by mid and end of the twenty-first century under RCP4.5 (blue) and RCP8.5 scenarios (red). Solid lines represent the means of the ensembles of RCMs



completed for two future 20-year periods (2031–2050 and 2080–2099) with respect to the reference period (1989–2008) under the RCP4.5 and RCP8.5 emission scenarios to better understand the future climatic condition in Syria.

At the 20-year annual mean, we found that the analysed mini-ensemble of five RCMs generally simulated the spatial pattern of the four variables mentioned quite well compared to the reference observational data sets for the reference period. More pronounced biases were found at the seasonal time scale. In particular, remarkable differences were found for the seasonal means of temperature and precipitation for RCA4 and RegCM simulations (e.g., JJA and SON). The annual cycles derived from the areal averages of the monthly means for the four variables showed that most models were able to capture the main characteristics of the annual cycle over the region of interest, except for RegCM. RegCM showed a strong overestimation of precipitation during the summer months (when observations indicate a remarkable minimum of precipitation). Our results indicate the need for possible further tuning of RegCM over the Syrian region.

RCMs and additional observations were also analysed in the form of Taylor plots. The spatial correlations with the reference observational data set were around 0.95 for certain variables (see Fig. 6). The additional observational data sets analysed (ERA5 and Clara) did not always provide substantial added value to the RCMs.

The projected future changes of the analysed variables by mid-century and by far future are consistent under both RCPs (moderate scenario (RCP4.5) and high emission scenario (RCP8.5)). It should be noted that larger changes are projected following the RCP8.5 scenario.

Regional climate model projections also indicate a prevailing decrease in cloud cover and precipitation, an increase in temperature, and mixed results for solar

irradiance over Syria. We would like to highlight that regions with high solar irradiance in the reference period (e.g., the eastern and south-eastern regions) will continue to have this characteristic in the mid- and late-century. Therefore, based on our results, such regions would be suitable for future solar farm investments.

All of the simulations used in this study agreed on a progressive warming over Syria. By the end of the twenty-first century, the mean temperature is projected to increase by between 1.8 °C (under RCP4.5) and 6 °C (RCP8.5) compared to 1989–2008.

Given the projected regional climate change signals derived from the climate variables analysed, the people of Syria will face with a warmer and more arid climate by the end of the twenty-first century. These changes are associated with an increase in the frequency of weather-related extremes, but more research is needed to confirm this.

The results of this study emphasise the need to validate the data from RCM simulations and evaluate their performance when used for impact studies. The present research also provides an analysis of the impacts of climate change on the Syrian region. Accordingly, our research is one of the very first attempts to analyse climate change projections obtained from medium resolution (0.44°) RCM simulations accomplished over regions encompassing Syria.

Acknowledgements The authors would like to mention that the maps used in this research (which were prepared by the authors) are based on OpenStreetMaps and USGS data. All CORDEX data provided by the modelling groups for the MENA, AFR and WAS CORDEX regions are acknowledged and are available on the following website: <https://esgf-data.dkrz.de/search/esgf-dkrz/>.

Funding Open access funding provided by Eötvös Loránd University. The research was supported by the Hungarian Scientific Research Fund (OTKA FK-142349). Open access publication made possible by the agreement between EISZ (the national electronic information service in Hungary) and Springer Nature.

Declarations

Conflict of interest The Authors declare no conflict of interest.

Open Access This article is licensed under a Creative Commons Attribution 4.0 International License, which permits use, sharing, adaptation, distribution and reproduction in any medium or format, as long as you give appropriate credit to the original author(s) and the source, provide a link to the Creative Commons licence, and indicate if changes were made. The images or other third party material in this article are included in the article's Creative Commons licence, unless indicated otherwise in a credit line to the material. If material is not included in the article's Creative Commons licence and your intended use is not permitted by statutory regulation or exceeds the permitted use, you will need to obtain permission directly from the copyright holder. To view a copy of this licence, visit <http://creativecommons.org/licenses/by/4.0/>.

References

- Abbass K, Qasim MZ, Song H, Murshed M, Mahmood H, Younis I (2022) A review of the global climate change impacts, adaptation, and sustainable mitigation measures. *Environ Sci Pollut Res* 29:42539–42559. <https://doi.org/10.1007/s11356-022-19718-6>
- Almazroui M (2012) Dynamical downscaling of rainfall and temperature over the Arabian Peninsula using RegCM4. *Clim Res* 52:49–62
- Almazroui M, Sajjad Saeed M, Nazrul Islam M, Khalid S, Abdulrahman K, Alkhalaf RD (2017) Assessment of uncertainties in projected temperature and precipitation over the Arabian Peninsula: a comparison between different categories of CMIP3 models. *Earth Syst Environ*. <https://doi.org/10.1007/s41748-017-0012-z>
- Arab Center for the Studies of Arid Zones and Dry Lands (ACSAD). Drought vulnerability in the Arab region: case study - Drought in Syria, ten years of scarce water (2000–2010), 2011. https://www.unisdr.org/files/23905_droughtsyriasmall.pdf
- Betts RA, Alfieri L, Bradshaw C, Caesar J, Feyen L, Friedlingstein P et al (2018) Changes in climate extremes, fresh water availability and vulnerability to food insecurity projected at 1.5°C and 2°C global warming with a higher-resolution global climate model, *philosophical transactions of the royal society a: mathematical. Phys Eng Sci* 376(2119):20160452. <https://doi.org/10.1098/rsta.2016.0452>
- Christensen OB, Christensen JH, Machehauer B, Botzet M (1998) Very high-resolution regional climate simulations over Scandinavia—present climate. *J Clim* 11:3204–3229. [https://doi.org/10.1175/1520-0442\(1998\)011%3c3204:VHRRC%3e2.0.CO;2](https://doi.org/10.1175/1520-0442(1998)011%3c3204:VHRRC%3e2.0.CO;2)
- Ciarlo JM, Coauthors (2021) A new spatially distributed added value index for regional climate models: the EURO-CORDEX and the CORDEX-CORE highest resolution ensembles. *Clim Dyn* 57:1403–1424. <https://doi.org/10.1007/s00382-020-05400-5>
- Clarke ED, Griffin S, McDermott F, Correia J, Sweeney C (2021) Which reanalysis dataset should we use for renewable energy analysis in Ireland. *Atmosphere* 12(5):624. <https://doi.org/10.3390/ATMOS12050624>
- Cornes R, van der Schrier G, van den Besselaar EJM, Jones PD (2018) An ensemble version of the E-OBS temperature and precipitation datasets. *J Geophys Res Atmos*. <https://doi.org/10.1029/2017JD028200>
- Déqué M, Rowell DP, Lüthi D et al (2007) An intercomparison of regional climate simulations for Europe: assessing uncertainties in model projections. *Clim Change* 81(1):53–70. <https://doi.org/10.1007/s10584-006-9228-x>
- Diro GT, Sushama L (2017) The role of soil moisture-atmosphere interaction on future hot spells over North America as simulated by the Canadian regional climate model (CRCM5). *J Clim* 30(13):5041–5058
- Dudney J, Suding KN (2020) The elusive search for tipping points. *Nat Ecol Evol* 4:1449–1450. <https://doi.org/10.1038/s41559-020-1273-8>
- Dutta R, Chanda K, Maity R (2022) Future of solar energy potential in a changing climate across the world: A CMIP6 multi-model ensemble analysis. *Rene Energy*. <https://doi.org/10.1016/j.renene.2022.02.023>
- Eyring V, Bony S, Meehl GA et al (2016) Overview of the coupled model intercomparison project phase 6 (CMIP6) experimental design and organization. *Geosci Model Dev* 9:1937–1958. <https://doi.org/10.5194/gmd-9-1937-2016>
- Faour G, Meslmani Y, Fayad A (2010) Climate-Change Atlas of Syria. <https://doi.org/10.13140/RG.2.2.26562.17601>
- Food and Agriculture Organization of the United Nations (FAO). Global forest resources assessment: Country report—Syrian Arab Republic, 2014. <http://www.fao.org/3/a-az348e.pdf>
- Food and Agriculture Organization of the United Nations (FAO). Syrian Arab Republic: Precipitation analysis, 1980–2021. Rome, 2021. Doi: <https://doi.org/10.4060/cb7151en>.
- Forster PM, Maycock AC, McKenna CM, Smith CJ (2020) Latest climate models confirm need for urgent mitigation. *Nat Climate Change* 10:7–10. <https://doi.org/10.1038/s41558-019-0660-0>
- Giorgi F (2019) Thirty years of regional climate modelling: where are we and where are we going next? *J Geophys Res: Atmospheres* 124:5696–5723. <https://doi.org/10.1029/2018JD030094>
- Giorgi F, Bi X (2000) A study of internal variability of a regional climate model. *J Geophys Res* 105(24):29503–29521. <https://doi.org/10.1029/2000JD900269>
- Giorgi F, Jones C, Asrar G (2009) Addressing climate information needs at the regional level: the CORDEX framework. *WMO Bulletin* 58:175–183
- Giorgi F, Coppola E, Solmon F, Mariotti L, Sylla MB, Bi X, Elguindi N, Diro GT, Nair V, Giuliani G, Turuncoglu UU, Cozzini S, Güttler I, O'Brien TA, Tawfik AB, Shalaby A, Zakey AS, Steiner AL, Stordal F, Sloan LC, Branković C (2012) RegCM4: model description and preliminary tests over multiple CORDEX domains. *Climate Res* 52:7–29. <https://doi.org/10.3354/cr0101018>
- Gutowski WJ, Giorgi F, Timbal B, Frigon A, Jacob D et al (2016) WCRP Coordinated Regional Downscaling Experiment (CORDEX): a diagnostic MIP for CMIP6. *Eur Geosci Union Geosci Model Devel Discuss* 11:4087–4095
- Harari M, Ferrara EL (2018) Conflict, climate, and cells: a disaggregated analysis. *Rev Econ Stat* 100(4):594–608. https://doi.org/10.1162/rest_a_00730
- Harris I, Osborn TJ, Jones P et al (2020) Version 4 of the CRU TS monthly high-resolution gridded multivariate climate dataset. *Sci Data* 7:109. <https://doi.org/10.1038/s41597-020-0453-3>
- Hassan M, Du P, Jia S, Iqbal W, Mahmood R, Ba W (2015) An assessment of the South Asian summer monsoon variability for present and future climatologies using a high resolution regional climate model (RegCM4.3) under the AR5 scenarios. *Atmos* 6(11):1833–1857
- Hersbach H, Bell B, Berrisford P, Biavati G, Horány A, Muñoz SJ, Nicolas J, Peubey C, Radu R, Rozum I, Schepers D, Simmons A, Soci C, Dee D, Thépaut J-N (2019) ERA5 monthly averaged data on pressure levels from 1959 to present. *Cop Clim Change Ser*. <https://doi.org/10.24381/cds.6860a573>
- Hoffmann L, Günther G, Li D, Stein O, Wu X, Griessbach S, Heng Y, Konopka P, Müller R, Vogel B, Wright JS (2019) From ERA-Interim to ERA5: the considerable impact of ECMWF's next-generation reanalysis on Lagrangian transport simulations. *Atmos Chem Phys* 19:3097–3124. <https://doi.org/10.5194/acp-19-3097-2019>

- IPCC (2013) Climate Change 2013: The Physical Science Basis. In: Stocker TF, Qin D, Plattner G-K, Tignor MMB, Allen SK, Boschung J, Nauels A, Xia Y, Bex V, Midgley PM (eds) Contribution of Working Group I to the Fifth Assessment Report of the Intergovernmental Panel on Climate Change. Cambridge University Press, Cambridge, United Kingdom and New York, NY, USA, 1535. <https://doi.org/10.1017/CBO9781107415324>
- IPCC (2015) Special report global warming of 1.5°C, annex I: glossary
- IPCC (2023) Climate Change 2023: Synthesis Report. A Report of the Intergovernmental Panel on Climate Change. In: Core Writing Team, H. Lee and J. Romero (eds) Contribution of Working Groups I, II and III to the Sixth Assessment Report of the Intergovernmental Panel on Climate Change. IPCC, Geneva, Switzerland, (in press)
- Jacob D (2001) A note to the simulation of the annual and inter-annual variability of the water budget 15 over the Baltic Sea drainage basin. *Meteorol Atmos Phys* 77(61–73):3088
- Karlsson, Karl-Göran; Anttila, Kati; Trentmann, Jörg; Stengel, Martin; Solodovnik, Irina; Meirink, Jan Fokke; Devasthale, Abhay; Kothe, Steffen; Jääskeläinen, Emmihenna; Sedlar, Joseph; Benas, Nikos; van Zadelhoff, Gerd-Jan; Stein, Diana; Finkensieper, Stephan; Håkansson, Nina; Hollmann, Rainer; Kaiser, Johannes; Werscheck, Martin (2020): CLARA-A2.1: CM SAF cloud, Albedo and surface Radiation dataset from AVHRR data - Edition 2.1, Satellite Application Facility on Climate Monitoring, DOI:https://doi.org/10.5676/EUM_SAF_CM/CLARA_AVHRR/V002_01
- Karnieli A, Shtein A, Panov N, Weisbrod N, Tal A (2019) Was drought really the trigger behind the syrian civil war in 2011? *Water* 11:1564. <https://doi.org/10.3390/w11081564>
- Kelley, Colin P. 2015. "Climate Change in the Fertile Crescent and Implications of the Recent Syrian Drought." *PNAS*. <http://www.pnas.org/content/112/11/3241.full.pdf?with-ds=yes>
- King D, Schrag D, Dadi Z, Qui Y, Ghosh A (2015) Climate change: a risk assessment. Cambridge University Centre for Science and Policy, Cambridge
- Kotlarski S, Keuler K, Christensen OB, Colette A, Déqué M, Gobiet A, Goergen K, Jacob D, Lüthi D, van Meijgaard E, Nikulin G, Schär C, Teichmann C, Vautard R, Warrach-Sagi K, Wulfmeyer V (2014) Regional climate modeling on European scales: a joint standard evaluation of the EURO-CORDEX RCM ensemble. *Geosci Model Dev* 7:1297–1333. <https://doi.org/10.5194/gmd-7-1297-2014>
- Kupiainen M, Samuelsson P, Jones C, Jansson C, Willén U, Hansson U, Ullerstig A, Wang S, Döscher R (2011) Rossby Centre Regional Atmospheric Model, RCA4. Rossby Centre Newsletter, The Rossby Centre Regional Climate model RCA3 model description and performance Doi: <https://doi.org/10.3402/tellusa.v63i1.15770>
- Mansour Almazroui M, Islam N, Saeed S, Alkhalaf AK, Dambul R (2017) Assessment of uncertainties in projected temperature and precipitation over the arabian peninsula using three categories of cmip5 multimodel ensembles. *Earth Syst Environ* 1:23. <https://doi.org/10.1007/s41748-017-0027-5>
- Mansour Almazroui M, Islam N, Saeed S et al (2020) Future changes in climate over the arabian peninsula based on CMIP6 multimodel simulations. *Earth Syst Environ* 4:611–630. <https://doi.org/10.1007/s41748-020-00183-5>
- Massoud Ali (2010) Years of Drought: A Report on the Effects of Drought on the Syrian Peninsula. Heinrich-Böll-Stiftung - Middle East Office. https://lb.boell.org/sites/default/files/uploads/2010/12/drought_in_syria_en.pdf
- Meng Y, Liu J, Leduc S, Mesfun S, Kraxner F, Mao G et al (2020) Hydropower production benefits more from 15°C than 2°C climate scenario. *Water Res Res* 56:025519. <https://doi.org/10.1029/2019WR025519>
- Moalaffi DB, Evans JP, Sharma A (2017) Influence of reanalysis datasets on dynamically downscaling the recent past. *Clim Dyn* 49:1239–1255. <https://doi.org/10.1007/s00382-016-3378-y>
- Moss RH, Edmonds JA, Hibbard KA, Manning MR, Rose SK, van Vuuren DP, Carter TE, Emori S, Kainuma M, Kram T, Meehl GA, Mitchell JFB, Nakicenovic N, Riahi K, Smith SJ, Stouffer RJ, Thomson AM, Weyant JP, Wilbanks TJ (2010) The next generation of scenarios for climate change research and assessment. *Nature* 463:747–756
- Mousa A (2011) Atmospheric irregularities in syria during (10–18 May, 2007). *Damascus Univer J* 27:3–4
- Ozturk T, Turp MT, Türkeş M, Kurnaz ML (2018) Future projections of temperature and precipitation climatology for CORDEX-MENA domain using RegCM4.4. *Atmos Res* 206:87–107
- Pfeifroth U, Sanchez-Lorenzo A, Manara V, Trentmann J, Hollmann R (2018) Trends and variability of surface solar radiation in Europe based on surface-and satellite-based data records. *J Geophys Res Atmos* 123(3):1735–1754
- Saravanan R (2022) The Climate Demon: Past, Present, and Future of Climate Prediction. Cambridge University Press, Cambridge, p 350
- Schulzweida Uwe (2021) CDO User Guide (Version 2.0.0). Zenodo
- Simmons A, Uppala S, Dee D, Kobayashi S (2006) ERA-Interim: New ECMWF reanalysis products from 1989 onwards. *ECMWF Newsletter* 110:26–35. <https://doi.org/10.21957/pocnex23c6>
- Sun Y, Hu T, Zhang X, Li C, Lu C, Ren G, Jiang Z (2019) Contribution of global warming and urbanization to changes in temperature extremes in Eastern China. *Geophys Res Lett* 46:11426–11434. <https://doi.org/10.1029/2019GL084281>
- Sutton RT (2019) Climate science needs to take risk assessment much more seriously. *Bull Am Meteorol Soc* 100(9):1637–1642
- Tapiador FJ, Navarro A, Moreno R, Luis SJ, Garcia-Ortega E (2020) Regional climate models: 30 years of dynamical downscaling *Atmos. Res.* <https://doi.org/10.1016/j.atmosres.2019.104785>
- Taylor KE (2001) Summarising multiple aspects of model performance in a single diagram. *J Geophys Res* 106:7183–7192. <https://doi.org/10.1029/2000JD900719>
- Taylor KE, Stouffer RJ, Meehl GA (2012) An overview of CMIP5 and the experiment design. *Bull Am Meteorol Soc* 93:485–498
- Torma C, Coppola E, Giorgi F, Bartholy J, Pongrácz R (2011) Validation of a high resolution version of the regional climate model RegCM3 over the Carpathian Basin. *J Hydrometeorol* 12:84–100
- Torma C, Giorgi F, Coppola E (2015) Added value of regional climate modeling over areas characterized by complex terrain—Precipitation over the Alps. *J Geophys Res Atmos* 120:3957–3972. <https://doi.org/10.1002/2014JD022781>
- United Nations Economic and Social Commission for Western Asia (ESCWA). Arab Climate Change Assessment Report—Main Report; E/ESCWA/SDPD/2017/RICCAR/Report; United Nations Economic and Social Commission for Western Asia (ESCWA): Beirut, Lebanon, 2017
- United States Agency for International Development (USAID). Climate change risk profile: Syria—Country overview, 2017. https://www.climatechange.org/sites/default/files/asset/document/2017_USAID_GEMS_Climate%20Change%20Risk%20Profile_Syria.pdf
- van Meijgaard E, van Ulft LH, Lenderink G, de Roode SR, Wipfler EL, Boers R, van Timmermans RMA (2012) Refinement and application of a regional atmospheric model for climate scenario calculations of Western Europe. *Clim Changes Spat Plann Publ* 054(12):46
- Wang J, Swati FNU, Stein ML, Kotamarthi VR (2015) Model performance in spatiotemporal patterns of precipitation: new methods

- for identifying value added by a regional climate model. *J Geophys Res* 120(4):1239–1259
- World Bank, The Climate Change Knowledge Portal (CCKP) for development practitioners and policy makers (CCKP). Available at: <https://climateknowledgeportal.worldbank.org/>. Accessed 28 Sept 2022.
- Yang T, Liu X, Wang L, Bai P, Li J (2020) Simulating hydropower discharge using multiple decision tree methods and a dynamical model merging technique. *J Water Res Plann Manag.* 146(2):055007. [https://doi.org/10.1061/\(ASCE\)146\(2\):055007](https://doi.org/10.1061/(ASCE)146(2):055007).
- Zhang X, Alexander L, Hegerl GC, Jones P, Tank AK, Peterson TC, Zwiers FW (2011) Indices for monitoring changes in extremes based on daily temperature and precipitation data. *Wiley Interdiscipl Rev: Clim Chan* 2(6):851–870. <https://doi.org/10.1002/wcc.147>
- Zheng HY, Miao CY, Wu JW, Lei XH, Liao WH, Li H (2019) Temporal and spatial variations in water discharge and sediment load on the Loess Plateau, China: a high-density study. *Sci Total Environ* 666:875–886. <https://doi.org/10.1016/j.scitotenv.2019.02.246>